

Label Information Guided Graph Construction for Semi-Supervised Learning

Liansheng Zhuang, *Member, IEEE*, Zihan Zhou, *Member, IEEE*, Shenghua Gao, Jingwen Yin, Zhouchen Lin, *Senior Member, IEEE*, and Yi Ma, *Fellow, IEEE*

Abstract—In the literature, most existing graph-based semi-supervised learning methods only use the label information of observed samples in the label propagation stage, while ignoring such valuable information when learning the graph. In this paper, we argue that it is beneficial to consider the label information in the graph learning stage. Specifically, by enforcing the weight of edges between labeled samples of different classes to be zero, we explicitly incorporate the label information into the state-of-the-art graph learning methods, such as the low-rank representation (LRR), and propose a novel semi-supervised graph learning method called semi-supervised low-rank representation. This results in a convex optimization problem with linear constraints, which can be solved by the linearized alternating direction method. Though we take LRR as an example, our proposed method is in fact very general and can be applied to any self-representation graph learning methods. Experiment results on both synthetic and real data sets demonstrate that the proposed graph learning method can better capture the global geometric structure of the data, and therefore is more effective for semi-supervised learning tasks.

Index Terms—Label information, low-rank representation, semi-supervised graph learning.

I. INTRODUCTION

IN COMPUTER vision and machine learning research communities, semi-supervised learning (SSL) [1]–[3] has attracted numerous attention over the past decade because of its ability to make use of rich unlabeled data for training. It has been demonstrated that unlabeled data, when used in conjunction with a small set of labeled data, can often considerably improve the learning accuracy. Among the current methods, graph-based SSL is an appealing approach due to its low computation complexity and flexibility in practice.

In general, a graph-based SSL method consists of two key steps. First, a graph is built from all data samples

Manuscript received July 10, 2016; revised February 12, 2017 and April 12, 2017; accepted April 22, 2017. Date of publication May 18, 2017; date of current version June 23, 2017. This work was supported by the National Science Foundation of China under Grant 61472379 and Grant 61371192. The work of Z. Lin was supported in part by the National Basic Research Program of China (973 Program) under Grant 2015CB352502 and in part by the National Natural Science Foundation of China under Grant 6162530 and Grant 61231002. The associate editor coordinating the review of this manuscript and approving it for publication was Dr. Ivana Totic. (*Corresponding author: Liansheng Zhuang.*)

L. Zhuang and J. Yin are with the University of Science and Technology of China, Hefei 230027, China (e-mail: lszhuang@ustc.edu.cn).

Z. Zhou is with the College of Information Sciences and Technology, Pennsylvania State University, State College, PA 16801 USA.

S. Gao and Y. Ma are with ShanghaiTech University, Shanghai, China.

Z. Lin is with the Key Laboratory of Machine Perception (MOE), School of EECS, Peking University, Beijing 100871, China, and also with the Cooperative Medianet Innovation Center, Shanghai Jiao Tong University, Shanghai 200240, China.

Color versions of one or more of the figures in this paper are available online at <http://ieeexplore.ieee.org>.

Digital Object Identifier 10.1109/TIP.2017.2703120

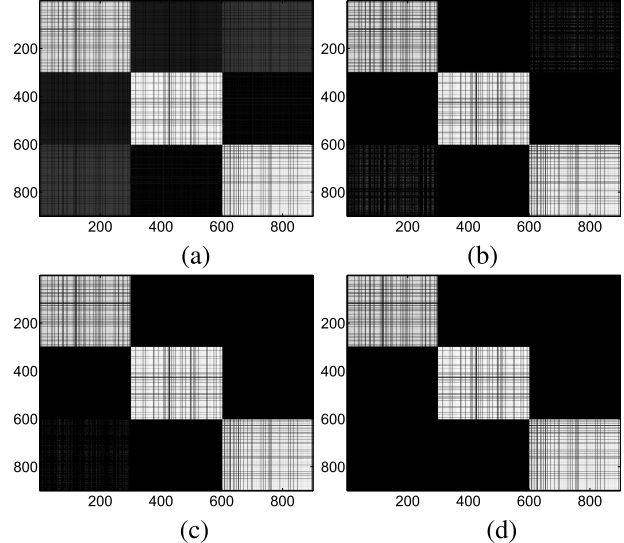


Fig. 1. Visualization of the unsupervised LRR-graph and semi-supervised SSLRR-graph with 10%, 30%, and 60% labeled data in a synthetic dataset. The “block-diagonal structure” of the graph is best preserved by the SSLRR-graph with 60% labeled data samples. (a) LRR-graph. (b) SSLRR-graph (10%). (c) SSLRR-graph (30%). (d) SSLRR-graph (60%).

(including both labeled and unlabeled samples) to model the relationships among the points. Then, label information of the labeled samples is propagated to the unlabeled samples over the graph. Though different graph-based SSL methods formulate the label propagation process via different objective functions, all of them share one common assumption (i.e., the *cluster assumption*), that is, points on the same structure (such as a cluster, a subspace, or a manifold) are likely to have the same label. Since one normally does not have an explicit model for the underlying structures, a graph constructed from the data samples often serves as an approximation to it. Therefore, constructing a good graph that best captures the essential data structure is critical for all graph-based SSL methods.

This paper proposes a novel framework to address the graph construction problem in SSL. Our key insight is that most graph-based SSL methods do not take advantage of label information when building a graph from the data samples, which limits their performance. Leveraging powerful tools from high-dimensional statistics and optimization, we successfully mitigate this issue by constructing the graph in a *semi-supervised* manner. Our framework is quite general and can be applied to many existing graph learning methods. As an example, Figure 1 compares the SSLRR-graphs constructed by our method to the original LRR-graph [4] on a synthetic dataset (see Section V-A about synthetic data generation).

A. Background and Motivations

Intuitively, a good graph should reveal the true intrinsic complexity or dimensionality of the data points by capturing the global structures of the data (i.e., multiple clusters, subspaces, or manifolds). Traditional methods such as *k-nearest neighbors* (*kNN*) and *Locality Linear Embedding* (*LLE*) [3], [5], [6], however, mainly rely on pair-wise Euclidean distance to build such a graph, thus are unable to capture the global data structures. As a result, these methods tend to be sensitive to local data noise and errors. Moreover, traditional methods always use fixed global parameters to determine the graph structure and the edge weights, thus may fail to offer any datum-adaptive neighborhoods.

Recently, motivated by the advance in fast computational methods in signal processing (particularly, in the areas of compressive sensing, sparse representation, and low-rank matrix recovery [7]–[11]), several methods [4], [12]–[15] have been proposed to construct undirected graphs that exploit the global structures of the data. Different from traditional methods, these methods seek a representation of each datum as a linear combination of *all* the other data samples. By solving a high-dimensional convex optimization problem, these methods automatically select the most informative “neighbors” for each datum, and simultaneously obtain the graph adjacency structure and weights in a nearly parameter-free fashion. We call these methods *self-representation methods*.

While the self-representation methods are datum-adaptive and robust to local errors, they also suffer from some problems in practice. In particular, in the ideal case, the linear coefficients recovered via convex optimization should be “structure-sparse”, that is, only those points belonging to the same structure as the target point should have nonzero coefficients. Unfortunately, this assumption only holds true if all the points lie in a union of independent or disjoint subspaces and are noiseless [16]. In other words, in the presence of dependent subspaces, nonlinear manifolds and/or data errors, these methods may select points from different structures (i.e., classes) to represent a data point, making the representation less informative.

To overcome this difficulty, our key insight is that all the aforementioned self-representation methods are *unsupervised*. That is, they do not utilize label information to learn the graph. Thus, when applied within the SSL framework, they could be further improved. To see why the label information provides valuable cues to the graph construction, consider the extreme case where the label information of all samples is available. In such case, one can directly enforce the coefficients belonging to different classes to be zero, so that the resulting representation is naturally structure-sparse. In fact, some researchers have explored the label information in graph construction [17]–[19]. However, these works are based on traditional graph construction methods, hence inevitably inherit the limits of traditional methods as mentioned above.

B. Our Contributions

Inspired by the above observations, we propose to explicitly incorporate label information into the

self-representation methods. Specifically, we show that one can seamlessly integrate the label information of a subset of the samples into the state-of-the-art self-representation methods, such as the LRR-graph [4], by restricting the representation coefficients between labeled points from different classes to be zero. Intuitively, this information helps us prevent the structure-sparsity of the coefficients from being destroyed in challenging real world scenarios, i.e., small signal-to-noise ratio, dependent subspaces and/or nonlinear manifolds. Thus, by solving a convex optimization problem with linear constraints, we can obtain a new linear representation for each data point which respects the label information, and subsequently construct a graph that better captures the global data structures.

To verify the effectiveness of our method, we conduct extensive experiments on both simulation datasets and public real datasets for two important tasks, namely nonlinear manifolds clustering and semi-supervised classification. The experimental results clearly demonstrate that, compared to graphs constructed via existing unsupervised self-representation methods, the graphs constructed by our method are more robust to data errors, and more informative and discriminative in practice, especially in the cases of complex data structures (e.g., dependent subspaces and nonlinear manifolds).

In summary, we make the following contributions in this paper:

- 1) We present a novel semi-supervised graph learning framework which seamlessly integrates the label information of data samples into the state-of-the-art graph learning methods. Compared with the graphs learned by existing methods, graphs learned by our method better capture the global structure of the data, especially when the data is subject to noises, the subspaces are not independent, or the data points lie in nonlinear manifolds.
- 2) We apply our method to both manifold clustering and semi-supervised learning tasks, and empirically demonstrate that the label information helps preserve the block-diagonal structure of the coefficient matrix, so that the learned graph is more informative and robust to data noises in practice.
- 3) While we use LRR as a representative example to illustrate our semi-supervised graph learning method, our method is in fact quite general and can be easily applied to other self-representation graph learning methods. To this end, we conduct experiments with three existing graph learning methods, namely LRR-graph, ℓ_1 -graph [12] and non-negative low rank and sparse graph (NNLRS-graph) [14]. We demonstrate that one can significantly improve the performance of these methods by incorporating the label information.

The remainder of this paper is organized as follows. In Section III, we present our semi-supervised graph learning framework. We give details about how to construct the graph weight matrix in Section IV. Experiment results and analysis are presented in Section V. Finally, Section VI concludes our paper.

II. RELATED WORK

Compared to label inference, graph construction has attracted much less attention in the machine learning community until recent years [5], [20]–[23]. Traditionally, ϵ -neighborhood and k -Nearest Neighbors (k NN) are commonly used in graph based SSL methods. An ϵ -neighborhood graph is built by connecting all the data points whose distance are smaller than the threshold ϵ . These graphs are often sensitive to the chosen parameter ϵ and produce undesirable degree distribution (e.g., disconnected components or almost-complete graph). On the other hand, a k NN graph links each node to its k nearest neighbors. Compared to ϵ -neighborhood graphs, k NN graphs enjoy some favorable properties in choosing the parameters, and tend to perform better than ϵ -neighborhood graphs in practice [5]. Various unsupervised methods have been proposed to improve the k NN graph construction [5], [6], [22]–[26]. For example, Wang *et al.* [24] estimated the graph edge weights in a manner of multi-wise edges instead of pairwise edges. Jebara *et al.* [5] proposed to use b -matching to produce a balanced or regular graph, which ensures that each node in the graph has the same number of edges. Other works focus on efficient algorithms to find the k nearest neighbors [27]–[31]. But a common limitation of all above methods is that the neighbors are selected “locally”—the decision is only based on the individual relation between the reconstructed data point and the other data points. Such neighbors can only capture the local data structure and thus greatly limit the performance of graph based SSL methods.

To remedy the above issue, *self-representation methods* [4], [12], [13], [32]–[36] have become increasingly popular in recent years. For example, ℓ_1 -graph [12] proposes to encode each datum as a sparse representation of the other samples. It is shown to have several advantages in practice, including robustness to noise, sparsity for efficiency, and datum-adaptive neighborhood [12]. Since ℓ_1 -graph is purely based on numerical solutions, Zhou *et al.* [35] propose to exploit the geometric data structure via a k NN fused lasso graph. Additionally, Fang *et al.* [32] impose the auto-grouped effect in the ℓ_1 -graph by applying two sparse regularizations: Elastic net and Octagonal Shrinkage and Clustering Algorithm for Regression (OSCAR). Han *et al.* [34] and Han and Qin [36] use a reduced size dictionary to preserve the locality and the geometry structure for data clustering applications. Yang *et al.* [33] use the Graph Laplacian regularization to improve the quality of ℓ_1 -graph.

To further capture the global data structure, Liu *et al.* [4] propose the LRR-graph, which seeks a low-rank representation of the data. By jointly obtaining the representation of all the data under the low-rankness assumption, LRR-graph effectively impose global constraints on the data structure (e.g., multiple subspaces). Moreover, since each sample can be used to represent itself, there always exist a feasible solution for LRR-graph even if the data sampling is insufficient. These properties make LRR-graph a good candidate for various learning tasks including SSL. Extensions to the original LRR-graph include [14], [37], which further impose non-negative and sparse constraints on the low-rank

representation, [38], which incorporates a block-diagonal prior, and [39], which combines the low-rank representation with the kernel trick. Other works introduce various regularized terms so as to explicitly consider the cases where the data lie on non-linear manifolds [15], [40]–[42].

However, most self-representation methods ignore the label information of the data samples during graph construction. In this paper, we demonstrate how the label information can be integrated into the construction of LRR-graph, resulting in significant improvement on the performance of existing SSL methods. Further, our framework can be readily applied to other self-representation methods such as ℓ_1 -graph, Least Squares Representation [43], Correlation Adaptive Subspace Segmentation [44], Correntropy Induced ℓ_2 -graph [45], and the Smooth Representation [46].

III. SEMI-SUPERVISED GRAPH LEARNING

In this section, we use the LRR-graph [4] as a representative example to describe our semi-supervised graph learning framework. For completeness, we first give a brief overview of LRR.

A. Low-Rank Representation: An Overview

Low-Rank Representation (LRR) was originally proposed in [4] to segment data drawn from a union of multiple linear (or affine) subspaces. Specifically, given a set of sufficiently dense data vectors $X = [\mathbf{x}_1, \mathbf{x}_2, \dots, \mathbf{x}_n] \in \mathbb{R}^{d \times n}$ (each column is a sample) drawn from a union of k subspaces, LRR seeks the lowest-rank representation among all the candidates that represent each data vector as the linear combination of the data themselves. It proposes to solve the following high-dimensional convex optimization problem:

$$\begin{aligned} \min_{Z, E} \quad & \|Z\|_* + \lambda \|E\|_{2,1} \\ \text{s.t.} \quad & X = XZ + E, \end{aligned} \quad (1)$$

where $Z = [z_1, z_2, \dots, z_n]$ is the coefficient matrix with each z_i being the coefficients of \mathbf{x}_i . In addition, $\|\cdot\|_*$ is the nuclear norm, i.e., sum of singular values. The $\ell_{2,1}$ -norm of E , $\|E\|_{2,1} = \sum_{j=1}^n \sqrt{\sum_{i=1}^d (e_{ij})^2}$ where e_{ij} is the (i, j) -th element of matrix E , is used to model the sample-specific corruptions and outliers. Finally, the parameter $\lambda > 0$ is used to balance the effects of the two terms. It can be chosen according to properties of the two norms, or tuned empirically.

As shown in [4], when data are clean and sampled from independent subspaces, the optimal solution Z^* of (1) is block-diagonal (ignoring the E term). That is, for each \mathbf{x}_i , only those entries of z_i which correspond to data points in the same subspace as \mathbf{x}_i have nonzero values. In this way, LRR is able to capture the global structure (i.e., multiple subspaces) of the data. Further, by introducing the error term $\|E\|_{2,1}$, LRR achieves robust subspace segmentation results despite of corrupted data vectors or outliers. After solving the problem (1), we can define the affinity matrix W of an undirected graph as $W = (|Z^*| + |Z^{*T}|)/2$. Consequently, the undirected graph (called the LRR-graph) also captures the global structure of the data.

However, in real applications, the data is always subject to noises, the subspaces could be dependent, and the data could even lie in nonlinear manifolds. In these cases, the block-diagonal structure of Z^* is often destroyed. To overcome this difficulty and improve the performance of the LRR-graph, we next propose a novel method to generalize the LRR model within the SSL framework by taking into account the label information of observed samples.

B. Semi-Supervised Low-Rank Representation

In this subsection, we incorporate the label information of observed samples into the original LRR framework, and propose a new model called *Semi-Supervised Low-Rank Representation* (SSLRR). The key idea of SSLRR is to preserve the known global geometric structure of data when solving the LRR problem. Specially, since we still aim to group the samples into one cluster if and only if they lie on the same subspace, the collection of all coefficient vectors $Z = [z_1, z_2, \dots, z_n]$ should remain low-rank and have a block-diagonal structure as in LRR. As we have some labeled samples, we can directly enforce the coefficients Z_{ij} between two labeled data points from different clusters to be zero. Therefore, the SSLRR model solves the following problem:

$$\begin{aligned} & \min_{Z, E} \|Z\|_* + \lambda \|E\|_{2,1} \\ & \text{s.t. } X = XZ + E, \\ & \quad Z^T \mathbf{1} = \mathbf{1}, \\ & \quad Z_{ij} = 0, \quad \forall (i, j) \in \Omega, \end{aligned} \quad (2)$$

where $\mathbf{1}$ is an all-one vector, Ω is the set of edges between two labeled samples from different classes, whereby $(i, j) \in \Omega$ indicates that x_i and x_j are not in the same class. As we can see from (2), similar to LRR, SSLRR also seeks the lowest-rank representation Z^* among all the data points. Meanwhile, by enforcing $Z_{ij} = 0, \forall (i, j) \in \Omega$, it makes use of the label information to help prevent the block-diagonal structure of Z^* from being destroyed in real world scenarios. By enforcing the sum-to-one constraint on the rows of the weight matrix, we hope to obtain the invariance to translations. The same trick is also used by existing methods, such as the popular Locally Linear Embedding (LLE) [3]. Since the SSLRR problem (2) is convex, it can be efficiently solved by fast first-order optimization methods, as we describe next.

C. Solving SSLRR via LADMAP

Recently, various methods have been proposed to solve the low-rank and sparse matrix recovery problem. In this paper, we adopt the Linearized Alternating Direction Method with Adaptive Penalty (LADMAP) [47] for its efficiency. LADMAP is a general method for solving convex programs with linear constraints. At each iteration, it first approximates the augmented Lagrangian function by linearizing the quadratic term and adding a proximal term. Then, it minimizes over the approximated function to update variables alternately. To apply LADMAP to our problem, we first define the

linear mappings:

$$\begin{aligned} \mathcal{A}(Z) &= \begin{pmatrix} \text{vec}(XZ) \\ Z^T \mathbf{1} \\ \mathcal{P}_\Omega(Z) \end{pmatrix}, \quad \mathcal{B}(E) = \begin{pmatrix} \text{vec}(E) \\ \mathbf{0} \\ \mathbf{0} \end{pmatrix}, \\ \mathbf{c} &= \begin{pmatrix} \text{vec}(X) \\ \mathbf{1} \\ \mathbf{0} \end{pmatrix}, \end{aligned}$$

where $\text{vec}(\cdot)$ is the vectorization operator that stacks columns of a matrix into a vector. $\mathcal{P}_\Omega(Z)$ is the projection operator that extracts the entries in Z whose indices are in Ω . Then, Eq. (2) can be rewritten as:

$$\begin{aligned} & \min_{Z, E} \|Z\|_* + \lambda \|E\|_{2,1} \\ & \text{s.t. } \mathcal{A}(Z) + \mathcal{B}(E) = \mathbf{c}. \end{aligned} \quad (3)$$

Then, applying LADMAP ([47, Algorithm 1]) to the standard form (3) yields the following updating rules.

Updating Z: First, we update Z as:

$$Z_{k+1} = \arg\min_Z \|Z\|_* + \frac{\beta_k \eta_{\mathcal{A}}}{2} \|Z - \tilde{Z}_k\|_F^2, \quad (4)$$

where k is the iteration number,

$$\tilde{Z}_k = Z_k - \mathcal{A}^* (\mathbf{y}_k + \beta_k [\mathcal{A}(Z_k) + \mathcal{B}(E_k) - \mathbf{c}]) / (\beta_k \eta_{\mathcal{A}}),$$

$\beta_k > 0$ is the penalty parameter, $\eta_{\mathcal{A}}$ is a relaxation parameter that satisfies $\eta_{\mathcal{A}} > \|\mathcal{A}\|_2$, in which $\|\mathcal{A}\|_2 = \max_{Z \neq 0} \|\mathcal{A}(Z)\|_F / \|Z\|_F$ is the operator norm of \mathcal{A} , and \mathcal{A}^* is the adjoint operator of \mathcal{A} .

Here, we note that $\|\mathcal{A}\|_2 \leq \sqrt{\|X\|_2^2 + n + 1}$ and $\mathcal{A}^*(\mathbf{w}) = X^T \text{mtx}(\mathbf{w}_1) + \mathbf{1}\mathbf{w}_2^T + \mathcal{P}_\Omega^*(\mathbf{w}_3)$, where

$$\mathbf{w} = \begin{pmatrix} \mathbf{w}_1 \\ \mathbf{w}_2 \\ \mathbf{w}_3 \end{pmatrix}$$

and the lengths of \mathbf{w}_1 , \mathbf{w}_2 , and \mathbf{w}_3 are dn , n , and $|\Omega|$, respectively. Additionally, $\text{mtx}(\cdot)$ is the operator that reshapes an $dn \times 1$ vector into a $d \times n$ matrix, $\mathcal{P}_\Omega^*(\cdot)$ is the adjoint operator of $\mathcal{P}_\Omega(\cdot)$ which maps a $|\Omega| \times 1$ vector to an $n \times n$ matrix by inserting the entries of the vector at places of the matrix whose indices are in Ω . The rest of the entries of the matrix are all zeros. Roughly speaking, mtx and \mathcal{P}_Ω^* can be viewed as the inverse operations of vec and \mathcal{P}_Ω , respectively.

Finally, the subproblem (4) has a closed form solution given by singular value thresholding (SVT) [48]:

$$Z_{k+1} = \tilde{U}_k \max \left(\tilde{\Sigma}_k - (\beta_k \eta_{\mathcal{A}})^{-1} I, 0 \right) \tilde{V}_k^T, \quad (5)$$

where $\tilde{U}_k \tilde{\Sigma}_k \tilde{V}_k^T$ is the singular value decomposition (SVD) of \tilde{Z}_k .

Updating E: Next, we update E as:

$$E_{k+1} = \arg\min_E \lambda \|E\|_{2,1} + \frac{\beta_k \eta_{\mathcal{B}}}{2} \|E - \tilde{E}_k\|_F^2, \quad (6)$$

where

$$\tilde{E}_k = E_k - \mathcal{B}^* (\mathbf{y}_k + \beta_k [\mathcal{A}(Z_{k+1}) + \mathcal{B}(E_k) - \mathbf{c}]) / (\beta_k \eta_{\mathcal{B}}),$$

and $\eta_{\mathcal{B}} > 0$ is a relaxation parameter that satisfies $\eta_{\mathcal{B}} > \|\mathcal{B}\|_2$, in which $\|\mathcal{B}\|_2 = \max_{E \neq 0} \|\mathcal{B}(E)\|_F / \|E\|_F$ is the operator norm of \mathcal{B} , and \mathcal{B}^* is the adjoint operator of \mathcal{B} . We note that $\|\mathcal{B}\|_2 \leq 1$ and $\mathcal{B}^*(\mathbf{w}) = \text{mtx}(\mathbf{w}_1)$, where \mathbf{w}_1 is the sub-vector of \mathbf{w} consisting of the first dn entries of \mathbf{w} .

Finally, the subproblem (6) also has a closed form solution [4]. Let $\mathbf{e}_{k+1,i}$ and $\tilde{\mathbf{e}}_{k,i}$ be the i -th column of E_{k+1} and \tilde{E}_k , respectively, we have:

$$\mathbf{e}_{k+1,i} = \max(1 - \lambda / (\beta_k \eta_{\mathcal{B}} \|\tilde{\mathbf{e}}_{k,i}\|_2), 0) \tilde{\mathbf{e}}_{k,i}. \quad (7)$$

Updating \mathbf{y} : Third, the Lagrange multiplier \mathbf{y} is updated as:

$$\mathbf{y}_{k+1} = \mathbf{y}_k + \beta_k [\mathcal{A}(Z_{k+1}) + \mathcal{B}(E_{k+1}) - \mathbf{c}]. \quad (8)$$

Updating β : Fourth, the penalty β is updated adaptively as follows:

$$\beta_{k+1} = \min(\beta_{\max}, \rho \beta_k), \quad (9)$$

where

$$\rho = \begin{cases} \rho_0, & \beta_k \max(\sqrt{\eta_{\mathcal{A}}} \|Z_{k+1} - Z_k\|_F, \\ & \sqrt{\eta_{\mathcal{B}}} \|E_{k+1} - E_k\|_2) / \|\mathbf{c}\|_2 \leq \varepsilon_2, \\ 1, & \text{otherwise,} \end{cases} \quad (10)$$

where $\rho_0 \geq 1$ is a constant and $0 < \varepsilon_2 \ll 1$ is a threshold.

The algorithm is summarized in Algorithm 1, in which the above iteration stops when the convergence criteria are met. More details about LADMAP can be referenced to [47].

Computational Complexity: Though label information is integrated, our SSLRR model has the same computational cost as the original LRR model. Specially, the computational cost of Algorithm 1 is mainly determined by updating the variables Z , E , and \mathbf{y} . For ease of analysis, let r_X be the lowest rank for X we can find with our algorithm, and k denote the number of iterations. Without loss of generality, we assume the sizes of X are $d \times n$ ($d < n$) in the following. In each iteration, SVT is used to update the low-rank matrix whose total complexity is $O(r_X n^2)$ when we use partial SVD. Then we compute XZ_{k+1} as $((X\hat{U}_k)\hat{V}_k^T)$ and employ soft thresholding to update the sparse error matrix E with the total complexity of $O(r_X n^2)$. The complexity of updating the Lagrange multiplier \mathbf{y} is $O(dn)$. So, the total cost of Algorithm 1 is $O(2kr_X n^2 + dn) = O(kr_X n^2)$.

IV. GRAPH CONSTRUCTION VIA SEMI-SUPERVISED LOW-RANK REPRESENTATION

Given a data matrix X , let $G = (V, E)$ be a graph associated with a weight matrix $W = \{w_{ij}\}$, where $V = \{\mathbf{v}_i\}_{i=1}^n$ is the node set, $E = \{e_{ij}\}$ is the edge set, and w_{ij} is the weight of edge e_{ij} linking two nodes \mathbf{v}_i and \mathbf{v}_j . The problem of graph construction is to determine the graph weight matrix W . In this paper, we are primarily concerned about the estimation of an undirected graph with nonnegative weights.

After solving problem (2), we may obtain the optimal coefficient matrix Z^* . Since each data point is represented by all the other samples, Z^* naturally characterizes the relationships among samples. Further, the low rank term of (2) encourages the coefficients of samples coming from the same affine

Algorithm 1 LADMAP for Solving the SSLRR Problem

Input: Data matrix $X = [x_1, x_2, \dots, x_n] \in \mathbb{R}^{d \times n}$, balance parameter λ , and indices set Ω .

Steps:

- 1: Set parameters $0 < \varepsilon_1 \ll 1$, $0 < \varepsilon_2 \ll 1$, β_{\max} , $\rho_0 \in [1, 1.5]$, $\eta_{\mathcal{A}} = \|X\|_F^2 + n + 1$, $\eta_{\mathcal{B}} = 1$.
- 2: Initialize $Z_0 = 0$, $E_0 = 0$, $\mathbf{y}_0 = \mathbf{0}$, $\beta_0 \in (0, 1)$, $k \leftarrow 0$.
- 3: **Do**
- 4: Update Z by (5).
- 5: Update E by (7).
- 6: Update \mathbf{y} by (8).
- 7: Update β by (9).
- 8: **While** $\|\mathcal{A}(Z_{k+1}) + \mathcal{B}(E_{k+1}) - \mathbf{c}\|_2 > \varepsilon_1$ or $\beta_k \max(\sqrt{\eta_{\mathcal{A}}} \|Z_{k+1} - Z_k\|_F, \sqrt{\eta_{\mathcal{B}}} \|E_{k+1} - E_k\|_2) / \|\mathbf{c}\|_2 > \varepsilon_2$

Output: The optimal solution (Z_{k+1}, E_{k+1}) .

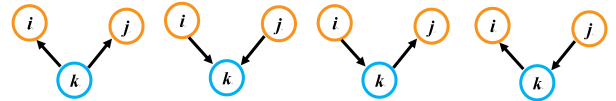


Fig. 2. Four fundamental second order processes on a directed graph [49]. From left to right: vertices i and j are co-cited by vertex k ; vertices i and j co-reference vertex k ; passage from vertices i to j ; passage from vertices j to i .

subspace to be highly correlated and fall into the same cluster, so that Z^* captures the global structure (i.e. the subspaces) of the whole data. However, the immediate output of SSLRR is a directed graph (asymmetric similarity between nodes). In order to make use of existing graph-based semi-supervised classification algorithms, a simple symmetrization step is often employed to convert the directed graph to an undirected one:

$$W = (|Z^*| + |Z^*|^T)/2. \quad (11)$$

However, the above step discards useful information conveyed by the edge directions. To preserve the valuable structural information from directed pairwise relationship between vertices, we adopt the Co-linkage Similarity (CS) [49], which considers a second-order random walk on the directed graph. The key idea is that, if from node i , a random walker has a higher probability to reach node j , then there is a larger similarity between i and j . To this end, [49] defines four types of process, i.e. co-citation, co-reference, passage ($i \rightarrow j$) and passage ($j \rightarrow i$) on a directed graph, as shown in Figure 2. Each type defines a similarity between vertex pairs on a directed graph. Thus, the effective similarity between two nodes on the directed graph is given by

$$W = Z^{*T} Z^* + Z^* Z^{*T} + Z^* Z^* + Z^{*T} Z^{*T}, \quad (12)$$

where the four terms represent co-citation, co-reference, passage ($i \rightarrow j$), and passage ($j \rightarrow i$), respectively. Clearly, the obtained graph weight matrix is symmetrical. Further, in this way we enhance the pairwise relationships between the vertices by taking into account the mutual link reinforcement and make the topological structure more lucid. We refer readers to Section V-C for an empirical comparison of the

Algorithm 2 Graph Construction via SSLRR

Input: Data matrix $X = [\mathbf{x}_1, \mathbf{x}_2, \dots, \mathbf{x}_n] \in \mathbb{R}^{d \times n}$, balance parameter λ .

Steps:

- 1: Normalize all the samples $\hat{\mathbf{x}}_i = \mathbf{x}_i / \|\mathbf{x}_i\|_2$ to obtain $\hat{X} = \{\hat{\mathbf{x}}_1, \hat{\mathbf{x}}_2, \dots, \hat{\mathbf{x}}_n\}$.
- 2: Assign the adjacency matrix Ω according to the label information of observed samples.
- 3: Solve the following problem by Algorithm 1:

$$(Z^*, E^*) = \arg \min_{Z, E} \|Z\|_* + \lambda \|E\|_1,$$

$$\text{s.t. } \hat{X} = \hat{X}Z + E, \mathbf{1}^T = \mathbf{1}^T Z,$$

$$Z_{ij} = 0, (i, j) \in \Omega.$$

- 4: Construct the graph weight matrix W by

$$W = Z^{*T} Z^* + Z^* Z^{*T} + Z^* Z^* + Z^{*T} Z^{*T}.$$

Output: The weight matrix W of SSLRR-graph.

TABLE I

THE SIX GRAPHS USED IN OUR EXPERIMENTS

Unsupervised	ℓ_1 -graph	LRR-graph	NNLRS-graph
Semi-Supervised	SSL1-graph	SSLRR-graph	SSNNLRS-graph

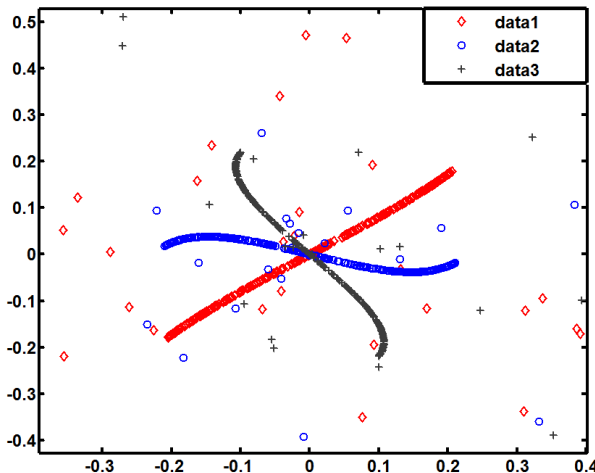


Fig. 3. An example of 900 points sampled in \mathbb{R}^2 and embedded in 100-D space with added noise and corruption.

graph weight matrix construction methods. More details about Co-linkage Similarity can be found in [49].

Finally, we summarize our method for constructing the SSLRR-graph in Algorithm 2.

V. EXPERIMENTS

To demonstrate the effectiveness of the proposed method, we conduct benchmark experiments in two scenarios, namely, manifold clustering on synthetic data and semi-supervised classification on real image data. Besides LRR, to further show the good generalization ability of the proposed semi-supervised graph learning framework, we adapt our method into two other existing self-representation methods:

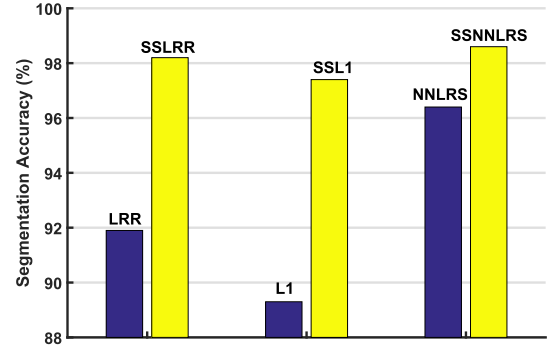


Fig. 4. Clustering results on the synthetic data.

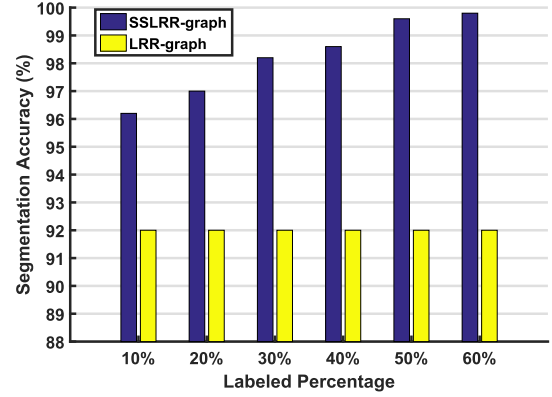
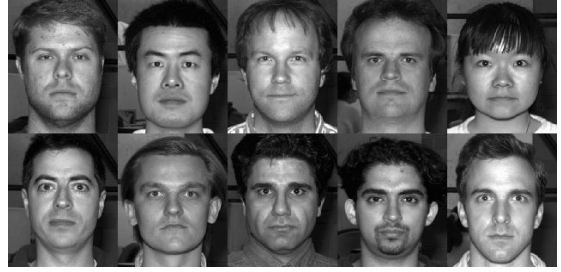


Fig. 5. Clustering results on the synthetic data with the variation of labeled percentage.



(a)



(b)

Fig. 6. Sample images in the PIE and YaleB face datasets. (a) PIE face images. (b) YaleB face images.

ℓ_1 -graph [12], and NNLRS-graph [14]. For these two methods, the label information is incorporated in the same way as in the LRR-graph.¹ We term the resultant methods as

¹Though there are other self-presentation methods (such as [13] and [15]), most of them are derived from ℓ_1 -graph and LRR-graph. Therefore, we choose ℓ_1 -graph, LRR-graph and NNLRS-graph as our reference methods.

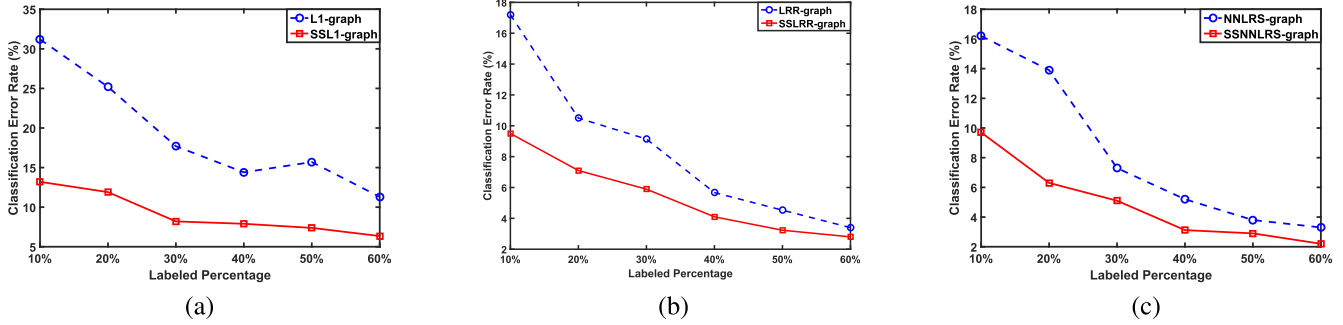


Fig. 7. Face recognition error rates on the YaleB dataset. (a) L1-graph vs SSL1-graph. (b) LRR-graph vs SSLR-graph. (c) NNLRS-graph vs SSNNLRS-graph.

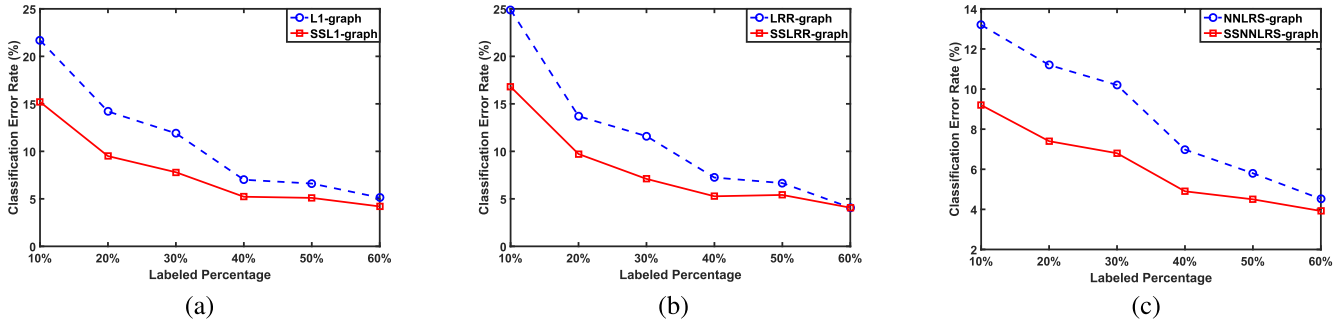


Fig. 8. Face recognition error rates on the PIE dataset. (a) L1-graph vs SSL1-graph. (b) LRR-graph vs SSLR-graph. (c) NNLRS-graph vs SSNNLRS-graph.

Semi-supervised ℓ_1 -graph (denoted as **SSL1-graph**) and *Semi-supervised NNLRS-graph* (denoted as **SSNNLRS-graph**), respectively. As a result, we have six graph learning methods in our experiments (three unsupervised methods and three semi-supervised methods), as shown in Table I.

Note that each semi-supervised graph learning method shares the same parameter as its corresponding unsupervised version. Specifically, for ℓ_1 -graph and SSL1-graph, as well as LRR-graph and SSLR-graph, one needs to choose the weight λ for the error term. For NNLRS-graph and SSNNLRS-graph, the parameters for the two error terms, β and λ , need to be determined. Compared to the unsupervised method, the only difference in the semi-supervised version is the additional constraint on the label information. Therefore, to better study the benefits of considering the label information in the graph learning stage, we decide to use the same parameter values for both methods in each experiment, and tune the parameters according to each dataset. Further, for fair comparison, we first tune the parameters for each unsupervised learning method, and then apply the same parameters to its semi-supervised version. In this way, we make sure that the choices of parameters do not favor our proposed semi-supervised methods.

A. Manifold Clustering on Synthetic Data

We consider the manifold clustering application by applying standard spectral clustering algorithm to the learned weight matrix W . The experiment is conducted on a series of synthetic data sets which contain Gaussian noises and data corruption. First, we evenly sample 900 noise-free points from three sinusoid manifolds. Then, the sample points are embedded into a 100-dimensional space and occupy the first two dimensions.



Fig. 9. Sample images in the USPS dataset.

We further add Gaussian noise with zero mean and variance 0.01 in all the 100 dimensions. Finally, we randomly select 10% of the samples and corrupt each sample with a much higher Gaussian noise with zero mean and variance $0.3\|\mathbf{x}\|_2$, where $\|\mathbf{x}\|_2$ is the ℓ_2 -norm of the sample. One example of the noisy data is shown in Figure 3.

After building six graphs with different methods, Normalized Cuts [50] is used for data segmentation. To apply the semi-supervised graph learning methods, we randomly select and label 30% of the observed samples from each cluster. As clustering methods do not provide the class label of each cluster, we use a post-processing step to assign each cluster a label: Given the ground truth classification results, the label of a cluster is the index of the ground truth class that contributes the maximum number of samples to the cluster. In this way, we can obtain the segmentation accuracy by computing the percentage of correctly classified samples, which is shown in Figure 4. It shows that the semi-supervised learning methods significantly outperform their unsupervised counterparts, suggesting that the label information can indeed improve the performance of self-representation graph learning methods.

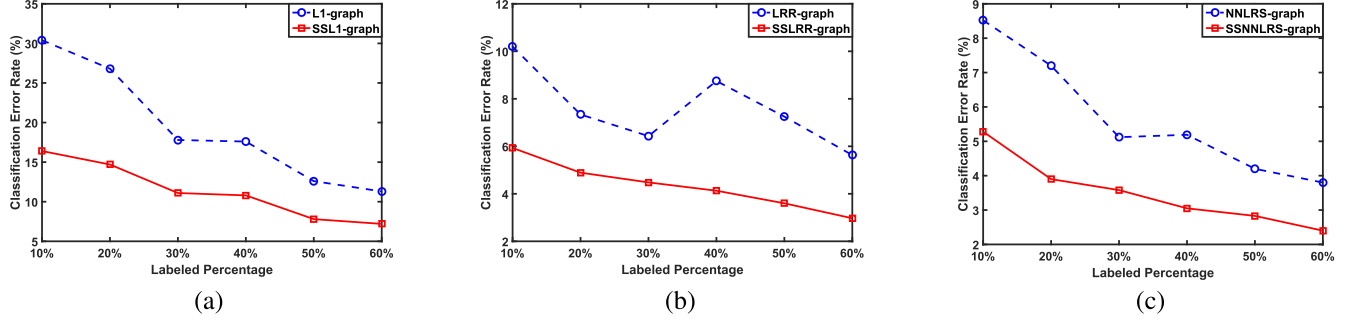


Fig. 10. Handwritten digit recognition error rates on the USPS dataset. (a) ℓ_1 -graph vs SSL1-graph. (b) LRR-graph vs SSLR-graph. (c) NNLRS-graph vs SSNNLRS-graph.

Sensitivity to the Percentage of Labeled Samples: To further evaluate the influence of label information, we vary the percentage of labeled samples from 10% to 60% for both LRR-graph and SSLR-graph. As shown in Figure 5, SSLR-graph consistently outperforms LRR-graph. In addition, the segmentation accuracy of SSLR-graph increases steadily as the percentage of labeled samples increases, resulting in a larger performance gap between these two methods. This suggests that adding more label information can help better preserve the underlying global data structures while we construct the graph. In Figure 1, we further visualize the graph weight matrix obtained by the LRR-graph and the SSLR-graph. As one can see, with the increase of the percentage of labeled samples, block-diagonal structure of the constructed graph becomes more evident.

B. Semi-Supervised Classification on Real Image Datasets

Besides synthetic data, we also evaluate our proposed semi-supervised graph-learning methods in applications including face recognition, handwritten digit recognition, and object recognition under the transductive learning setting. We adopt the popular *Local and Global Consistency* (LGC) [2] as the classification framework. Specifically, LGC builds upon an undirected graph, and utilizes the graph and known labels to recover a continuous classification function $F \in \mathbb{R}^{|V| \times c}$ by optimizing the following energy function:

$$\min_{F \in \mathbb{R}^{|V| \times c}} \text{tr}\{F^T L_w F + \mu(F - Y)^T (F - Y)\}, \quad (13)$$

where c is the number of classes, $Y \in \mathbb{R}^{|V| \times c}$ is the label matrix, in which $Y_{ij} = 1$ if sample x_i is associated with label j for $j \in \{1, 2, \dots, c\}$, and $Y_{ij} = 0$ otherwise. L_w is the normalized graph Laplacian $L_w = D^{-1/2}(D - W)D^{-1/2}$, in which D is a diagonal matrix with $D_{ij} = \sum_j W_{ij}$. The weight $\mu \in [0, \infty)$ balances the local fitting and the global smoothness of the function F . As suggested in [2], we fix $\mu = 0.01$ in all the experiments.

1) *Evaluation on Face Recognition:* We investigate the performance of our semi-supervised graph learning for face recognition on two well-known public face datasets: YaleB and CMU PIE. In the literature, both datasets have been frequently used to evaluate the performance of semi-supervised learning methods. The YaleB face database consists of 38 individuals, and each subject has around 64 near frontal images

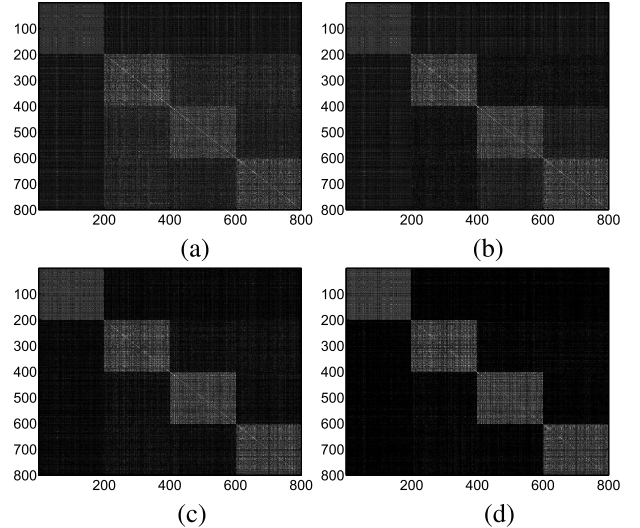


Fig. 11. Visualization of unsupervised LRR-graph and semi-supervised SSLR-graph with 10%, 30%, and 60% of labeled data from USPS database. (a) LRR-graph. (b) SSLR-graph (10%). (c) SSLR-graph (30%). (d) SSLR-graph (60%).



Fig. 12. Sample images in the COIL dataset.

under different illuminations. We use the cropped images of first 15 individuals for our experiment, and resize them to 32×32 pixels. The PIE face database contains 41368 images of 68 people, each person under 13 different poses, 43 different illumination conditions and with 4 different expressions. In our experiments, we only use the frontal images with neural

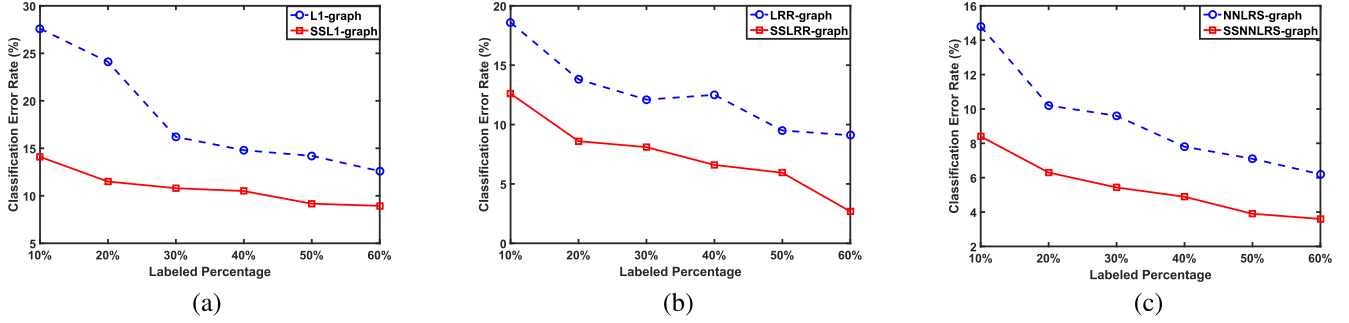


Fig. 13. Visual object recognition error rates on the COIL20 dataset. (a) ℓ_1 -graph vs SSL1-graph. (b) LRR-graph vs SSLRR-graph. (c) NNLRS-graph vs SSNNLRS-graph.

expression of the first 20 individual. The images are cropped using affine transformations based on locations of the eyes and nose, and resize them to 100×100 pixels. Sample images from these two face datasets are shown in Figure 6. Empirically, we have found that images of each subject in YaleB and PIE has a roughly linear subspace structure.

In Figure 7 and Figure 8, we report the classification accuracy based on six different graph learning methods on YaleB and PIE datasets. The percentage of the labeled samples varies from 10% to 60%. As expected, in most cases, the classification error rates for all methods decrease with the increase of the percentage of labeled samples. More importantly, in all cases, the semi-supervised graph learning methods outperform their unsupervised counterparts. For example, by incorporating the labels of 10% data samples in YaleB into the ℓ_1 -graph, the classification error rate is reduced from 31.2% to 13.2%. This demonstrates the importance of incorporating label information in graph construction.

2) *Evaluation on Handwritten Digit Recognition*: In this experiment, we address the handwritten digit recognition problem on the USPS dataset. The dataset contains normalized grey scale images of size 16×16 , divided into a training set of 7291 images and a test set of 2007 images. Following the setting of previous works, we only use the images of digits 1, 2, 3, and 4 as the four classes, which have 1296, 926, 824 and 852 samples, respectively. Some sample images from USPS digit dataset are shown in Figure 9.

Figure 10 shows the recognition error rates of all the six methods on the USPS dataset. As we can see, the proposed semi-supervised graph learning methods consistently outperform the unsupervised versions. Moreover, as the percentage of labeled samples increases, the classification error rates for SSL1-graph, SSLRR-graph, and SSNNLRR-graph decreases monotonically. This suggests that labeled samples help recover the underlying data structure of the learned graphs. In Figure 11, we further compare the weight matrices obtained by the LRR-graph and SSLRR-graph on USPS dataset. We can see that, with the increase of the number of labeled samples, the block-diagonal structure of the graphs is indeed better preserved.

3) *Evaluation on Visual Object Recognition*: We verify the importance of label information for graph learning for nonlinear manifolds by conducting visual object recognition

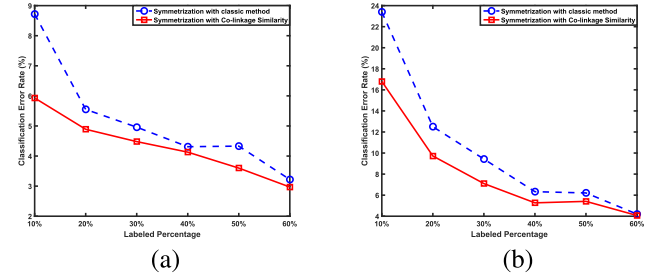


Fig. 14. Classification error rates using different graph weight matrix construction methods. (a) USPS. (b) PIE.

experiments on the COIL20 dataset. The dataset contains 20 objects. The images of each objects were taken 5 degrees apart as the object is rotated on a turntable, resulting in 72 images for each object. The size of the grayscale image is 32×32 pixels. Figure 12 shows some sample images in the COIL20 dataset. We have empirically found that data samples in the COIL20 dataset lie on non-linear manifolds. This makes the graph learning and classification tasks more challenging, because most self-representation methods (such as ℓ_1 -graph, LRR-graph, NNLRS-graph) are based on linear models.

Figure 13 reports the classification results of the six graph learning methods. As we can see, as the percentage of labeled samples increases, the classification error rates for our semi-supervised learning methods decrease. Further, they significantly outperform their corresponding unsupervised versions. For example, the error rate for LRR-graph on the COIL20 dataset with 60% labeled samples is 9.10%, whereas the error rate for SSLRR-graph is only 2.68%. This again demonstrates the importance of the incorporating label information in graph learning. By enforcing the weights between points from different categories to be zero, we can preserve part of the global data structure.

C. Influence of the Graph Construction Methods

In this subsection, we evaluate the influence of Co-linkage Similarity (CS) [49] on the graph construction. Taking SSLRR-graph as example, we use the classic method (i.e., Eq. (11)) and the Co-linkage Similarity (i.e., Eq. (12)) to symmetrize the directed graph, and obtain SSLRR-graph_{classic} and SSLRR-graph_{CS}, respectively.

We evaluate SSLRR-graph_{classic} and SSLRR-graph_{CS} under the same settings on both the USPS dataset and the PIE dataset. The classification error rate on these two datasets are shown in Figure 14. As we can see that, the Co-linkage Similarity does improve the performance of SSLRR-graph, especially when the percentage of labeled samples is small. Generally, as the labeled percentage increases, the influence becomes weaker.

VI. CONCLUSION

In this paper, we propose a new graph learning framework, which is able to obtain highly informative graphs for graph-based SSL methods. Different from existing graph learning methods, our method explicitly takes advantage of label information in both the graph learning and label propagation stages. In particular, by restricting the coefficient between any two labeled samples from different classes to be zero, our method seamlessly incorporates the label information of the data samples into any self-representation methods (e.g., ℓ_1 -graph, LRR-graph, and NNLRR-graph), and keep the same computational cost. As a result, the new graphs can better capture the global geometric structure of the data, therefore is more informative and discriminative, especially when the data is subject to noise, the subspaces are not independent, or the data points lie in nonlinear manifolds. Experiment results on both synthetic and real datasets demonstrate that the label information indeed helps preserve the block-diagonal structure of the coefficient matrices, and significantly improves the performance of existing graph learning methods.

As for future work, we plan to further investigate efficient algorithms for constructing large-scale SSLRR-graphs. Also, current methods conduct label propagation for classification after graph construction. It is interesting to develop principled method to solve the graph construction and label propagation problems at the same time.

REFERENCES

- [1] P. F. Felzenszwalb and D. P. Huttenlocher, "Efficient graph-based image segmentation," *Int. J. Comput. Vis.*, vol. 59, no. 2, pp. 167–181, 2004.
- [2] D. Zhou, O. Bousquet, T. Lal, J. Weston, and B. Scholkopf, "Learning with local and global consistency," in *Proc. NIPS*, 2004, pp. 595–602.
- [3] S. T. Roweis and L. K. Saul, "Nonlinear dimensionality reduction by locality linear embedding," *Science*, vol. 290, no. 5500, pp. 2323–2326, 2000.
- [4] G. Liu, Z. Lin, S. Yan, J. Sun, Y. Yu, and Y. Ma, "Robust recovery of subspace structures by low-rank representation," *IEEE Trans. Pattern Anal. Mach. Intell.*, vol. 35, no. 1, pp. 171–184, Jan. 2013.
- [5] T. Jebara, J. Wang, and S.-F. Chang, "Graph construction and b-matching for semi-supervised learning," in *Proc. ICML*, Jun. 2009, pp. 441–448.
- [6] D. Kong, C. H. Ding, H. Huang, and F. Nie, "An iterative locally linear embedding algorithm," in *Proc. 29th Int. Conf. Mach. Learn. (ICML)*, New York, NY, USA, 2012, pp. 1647–1654.
- [7] E. J. Candès and T. Tao, "Decoding by linear programming," *IEEE Trans. Inf. Theory*, vol. 51, no. 12, pp. 4203–4215, Dec. 2005.
- [8] D. L. Donoho, "Compressed sensing," *IEEE Trans. Inf. Theory*, vol. 52, no. 4, pp. 1289–1306, Apr. 2006.
- [9] M. Duarte *et al.*, "Single-pixel imaging via compressive sampling," *IEEE Signal Process. Mag.*, vol. 25, no. 2, pp. 83–91, Mar. 2008.
- [10] J. Wright, A. Y. Yang, A. Ganesh, S. S. Sastry, and Y. Ma, "Robust face recognition via sparse representation," *IEEE Trans. Pattern Anal. Mach. Intell.*, vol. 31, no. 2, pp. 210–227, Feb. 2009.
- [11] E. Candes, X. Li, Y. Ma, and J. Wright, "Robust principal component analysis?" *J. ACM*, vol. 58, no. 3, May 2011, Art. no. 11.
- [12] B. Cheng, J. Yang, S. Yan, Y. Fu, and T. Huang, "Learning with ℓ_1 -graph for image analysis," *IEEE Trans. Image Process.*, vol. 19, no. 4, pp. 858–866, Apr. 2010.
- [13] R. He, W.-S. Zheng, B.-G. Hu, and X.-W. Kong, "Nonnegative sparse coding for discriminative semi-supervised learning," in *Proc. CVPR*, Jun. 2011, pp. 792–801.
- [14] L. Zhuang, H. Gao, Z. Liu, Y. Ma, X. Zhang, and N. Yu, "Non-negative low rank and sparse graph for semi-supervised learning," in *Proc. CVPR*, Jun. 2012, pp. 2328–2335.
- [15] Y. Zheng, X. Zhang, S. Yang, and L. Jiao, "Low-rank representation with local constraint for graph construction," *Neurocomputing*, vol. 122, pp. 398–405, Dec. 2013.
- [16] R. Vidal, "Subspace clustering," *IEEE Signal Process. Mag.*, vol. 28, no. 2, pp. 52–68, Mar. 2011.
- [17] M. H. Rohban and H. R. Rabiee, "Supervised neighborhood graph construction for semi-supervised classification," *Pattern Recognit.*, vol. 45, no. 4, pp. 1362–1372, Apr. 2012.
- [18] L. Berton and A. de Andrade Lopes, "Graph construction based on labeled instances for semi-supervised learning," in *Proc. 22nd Int. Conf. Pattern Recognit. (ICPR)*, Aug. 2014, pp. 2477–2482.
- [19] P. S. Dhillon, P. P. Talukdar, and K. Crammer, "Inference driven metric learning (IDML) for graph construction," Dept. Comput. Inf. Sci., Univ. Pennsylvania, Philadelphia, PA, USA, Tech. Rep. MS-CIS-10-18, 2010.
- [20] M. Maier, U. von Luxburg, and M. Hein, "Influence of graph construction on graph-based clustering measures," in *Proc. NIPS*, 2008, pp. 1025–1032.
- [21] P. P. Talukdar, "Topics in graph construction for semi-supervised learning," Dept. Comput. Inf. Sci., Univ. Pennsylvania, Philadelphia, PA, USA, Tech. Rep. MS-CIS-09-13, Aug. 2009. [Online]. Available: http://repository.upenn.edu/cis_reports/936
- [22] D. A. Vega-Oliveros, L. Berton, A. M. Eberle, A. de Andrade Lopes, and L. Zhao, "Regular graph construction for semi-supervised learning," in *Proc. 2nd Int. Conf. Math. Modelling Phys. Sci.*, 2014, vol. 490, no. 1, Art. no. 012022.
- [23] L. Berton and A. de Andrade Lopes, "Graph construction for semi-supervised learning," in *Proc. 24th Int. Joint Conf. Artif. Intell. (IJCAI)*, 2015, pp. 4343–4344.
- [24] J. Wang, F. Wang, C. Zhang, H. C. Shen, and L. Quan, "Linear neighborhood propagation and its applications," *IEEE Trans. Pattern Anal. Mach. Intell.*, vol. 31, no. 9, pp. 1600–1615, Sep. 2009.
- [25] K. Ozaki, M. Shimbo, M. Komachi, and Y. Matsumoto, "Using the mutual k -nearest neighbor graphs for semi-supervised classification of natural language data," in *Proc. 15th Conf. Comput. Natural Lang. Learn.*, Jun. 2011, pp. 154–162.
- [26] M. Zhang, C. Ding, and D. Kong, "Collective kernel construction in noisy environment," in *Proc. SIAM Int. Conf. Data Mining (SMD)*, Austin, TX, USA, 2013, pp. 64–72.
- [27] Y.-M. Zhang, K. Huang, G. Geng, and C.-L. Liu, "Fast k NN graph construction with locality sensitive hashing," in *Proc. Joint Eur. Conf. Mach. Learn. Knowl. Discovery Databases*, 2013, pp. 660–674. [Online]. Available: http://dx.doi.org/10.1007/978-3-642-40991-2_42
- [28] W. Dong, C. Moses, and K. Li, "Efficient k -nearest neighbor graph construction for generic similarity measures," in *Proc. 20th Int. Conf. World Wide Web*, Apr. 2011, pp. 577–586.
- [29] D. C. Anastasiu and G. Karypis, "L2Knng: Fast exact k -nearest neighbor graph construction with L2-norm pruning," in *Proc. 24th ACM Int. Conf. Inf. Knowl. Manage. (CIKM)*, Oct. 2015, pp. 791–800.
- [30] Y. Park, S. Park, S.-G. Lee, and W. Jung, "Scalable k -nearest neighbor graph construction based on greedy filtering," in *Proc. 22nd Int. Conf. World Wide Web*, May 2013, pp. 227–228.
- [31] J. Wang, J. Wang, G. Zeng, Z. Tu, R. Gan, and S. Li, "Scalable k -NN graph construction for visual descriptors," in *Proc. CVPR*, Jun. 2012, pp. 1106–1113.
- [32] Y. Fang, R. Wang, B. Dai, and X. Wu, "Graph-based learning via auto-grouped sparse regularization and kernelized extension," *IEEE Trans. Knowl. Data Eng.*, vol. 27, no. 1, pp. 142–154, Jan. 2015.
- [33] Y. Yang, Z. Wang, J. Yang, J. Wang, S. Chang, and T. S. Huang, "Data clustering by laplacian regularized ℓ^1 -graph," in *Proc. AAAI*, Jul. 2014, pp. 3148–3149.
- [34] S. Han, H. Huang, H. Qin, and D. Yu, "Locality-preserving L_1 -graph and its application in clustering," in *Proc. 30th Annu. ACM Symp. Appl. Comput.*, Apr. 2015, pp. 813–818.
- [35] G. Zhou, Z. Lu, and Y. Peng, " L_1 -graph construction using structured sparsity," *Neurocomputing*, vol. 120, pp. 441–452, Nov. 2013.
- [36] S. Han and H. Qin, "Structure aware L_1 -graph for data clustering," in *Proc. AAAI*, Feb. 2016, pp. 4214–4215.

- [37] L. Zhuang *et al.*, "Constructing a nonnegative low-rank and sparse graph with data-adaptive features," *IEEE Trans. Image Process.*, vol. 24, no. 11, pp. 3717–3728, Nov. 2015.
- [38] J. Feng, Z. Lin, H. Xu, and S. Yan, "Robust subspace segmentation with block-diagonal prior," in *Proc. CVPR*, Jun. 2014, pp. 3818–3825.
- [39] S. Yang, Z. Feng, Y. Ren, H. Liu, and L. Jiao, "Semi-supervised classification via kernel low-rank representation graph," *Knowl.-Based Syst.*, vol. 69, pp. 150–158, Oct. 2014.
- [40] X. Lu, Y. Wang, and Y. Yuan, "Graph-regularized low-rank representation for destriping of hyperspectral images," *IEEE Trans. Geosci. Remote Sens.*, vol. 51, no. 7, pp. 4009–4018, Jul. 2013.
- [41] Y. Peng, B.-L. Lu, and S. Wang, "Enhanced low-rank representation via sparse manifold adaption for semi-supervised learning," *Neural Netw.*, vol. 65, pp. 1–17, May 2015.
- [42] L. Zhuang, J. Wang, Z. Liu, A. Yang, Y. Ma, and N. Yu, "Locality-preserving low-rank representation for graph construction from nonlinear manifolds," *Neurocomputing*, vol. 175, pp. 715–722, Jan. 2016.
- [43] C.-Y. Lu, H. Min, Z.-Q. Zhao, L. Zhu, D.-S. Huang, and S. Yan, "Robust and efficient subspace segmentation via least squares regression," in *Proc. ECCV*, 2012, pp. 347–360.
- [44] C. Lu, J. Feng, Z. Lin, and S. Yan, "Correlation adaptive subspace segmentation by trace lasso," in *Proc. ICCV*, Dec. 2013, pp. 1345–1352.
- [45] C. Lu, J. Tang, M. Lin, L. Lin, S. Yan, and Z. Lin, "Correntropy induced L₂ graph for robust subspace clustering," in *Proc. IEEE Int. Conf. Comput. Vis. (ICCV)*, Sydney, NSW, Australia, Dec. 2013, pp. 1801–1808.
- [46] H. Hu, Z. Lin, J. Feng, and J. Zhou, "Smooth representation clustering," in *Proc. CVPR*, Jun. 2014, pp. 3834–3841.
- [47] Z. Lin, R. Liu, and Z. Su, "Linearized alternating direction method with adaptive penalty for low rank representation," in *Proc. NIPS*, 2011, pp. 612–620.
- [48] J.-F. Cai, E. J. Candès, and Z. Shen, "A singular value thresholding algorithm for matrix completion," *SIAM J. Optim.*, vol. 20, no. 4, pp. 1956–1982, 2010.
- [49] H. Wang, H. Huang, and C. Ding, "Image categorization using directed graphs," in *Proc. ECCV*, 2010, pp. 762–775.
- [50] J. Shi and J. Malik, "Normalized cuts and image segmentation," *IEEE Trans. Pattern Anal. Mach. Intell.*, vol. 22, no. 8, pp. 888–905, Aug. 2000.



Liansheng Zhuang (M'10) received the bachelor's and Ph.D. degrees from the University of Science and Technology of China (USTC), China, in 2001 and 2006, respectively. In 2011, he was nominated to join the STARTRACKER Project of Microsoft Research of Asia (MSRA), and he was a Vendor Researcher with the Visual Computing Group, Microsoft Research, Beijing. From 2012 to 2013, he was a Visiting Research Scientist with the Department of EECS, University of California at Berkeley, Berkeley. He is currently an Associate Professor with the School of Information Science and Technology, USTC. His main research interest is in computer vision and machine learning. He is a member of ACM and CCF.

Professor with the School of Information Science and Technology, USTC. His main research interest is in computer vision and machine learning. He is a member of ACM and CCF.



Zihan Zhou (S'08–M'12) received the bachelor's degree in automation from Tsinghua University in 2007 and the Ph.D. degree in electrical and computer engineering from the University of Illinois at Urbana-Champaign in 2013. He is currently a Faculty Member with the College of Information Sciences and Technology, Pennsylvania State University. His research interest lies in computer vision, image processing, and machine learning.



Shenghua Gao received the B.E. degree from the University of Science and Technology of China in 2008 (outstanding graduates) and the Ph.D. degree from Nanyang Technological University in 2012. From 2012 to 2014, he was a Research Scientist with the Advanced Digital Sciences Center, Singapore. From 2015 to 2015, he visited UC Berkeley as a Visiting Scholar. He is currently an Assistant Professor with ShanghaiTech University, China. He has authored over 30 papers on object and face recognition related topics in many international conferences the IEEE T-PAMI, IJCV, the IEEE TIP, the IEEE TNNLS, the IEEE TMM, the IEEE TCSVT, CVPR, and ECCV. His research interests include computer vision and machine learning. He has organized tutorials in VCIP2015 and ACCV2014. He received the Microsoft Research Fellowship in 2010 and the ACM Shanghai Young Research Scientist in 2015. He was a recipient of the National 1000 Young Talents Program in 2016.



Jingwen Yin received the bachelor's degree from the University of Science and Technology of China in 2016. She is currently pursuing the master's degree with the Department of Computer Science, University of Southern California. Her research interest lies in machine learning and computer vision.



Zhouchen Lin (M'00–SM'08) received the Ph.D. degree in applied mathematics from Peking University in 2000. He was a Chair Professor with Northeast Normal University. He is currently a Professor with the Key Laboratory of Machine Perception (Ministry of Education), School of Electronics Engineering and Computer Science, Peking University. His research interests include computer vision, image processing, machine learning, pattern recognition, and numerical optimization. He is an IAPR Fellow. He is an Associate Editor of the IEEE

TRANSACTIONS ON PATTERN ANALYSIS AND MACHINE INTELLIGENCE and the *International Journal of Computer Vision*.



Yi Ma (F'13) received the bachelor's degree in automation and applied mathematics from Tsinghua University, Beijing, China, in 1995, and the M.Sc. degree in EECS, the M.A. degree in mathematics, and the Ph.D. degree in EECS from the University of California at Berkeley, in 1997, 2000, and 2000, respectively. From 2009 to 2014, he was a Principal Researcher and the Research Manager of the Visual Computing Group, Microsoft Research, Beijing. From 2000 to 2011, he was an Associate Professor with the Electrical & Computer Engineering Department, University of Illinois at Urbana–Champaign. He is currently a Professor and the Executive Dean of the School of Information and Science and Technology, ShanghaiTech University, China. He has authored two textbooks *An Invitation to 3-D Vision* (Springer, 2004), and *Generalized Principal Component Analysis* (Springer, 2016). His main research interest is in computer vision, high-dimensional data analysis, and systems theory. He received the David Marr Best Paper Prize at the International Conference on Computer Vision 1999, the Longuet-Higgins Best Paper Prize (honorable mention) at the European Conference on Computer Vision 2004, and the Sang Uk Lee Best Student Paper Award with his students at the Asian Conference on Computer Vision in 2009. He also received the CAREER Award from the National Science Foundation in 2004 and the Young Investigator Award from the Office of Naval Research in 2005. He served as the Program Chair for ICCV 2013 and the General Chair for ICCV 2015. He was an Associate Editor of the IEEE TRANSACTIONS ON PATTERN ANALYSIS AND MACHINE INTELLIGENCE, the *International Journal of Computer Vision*, and the IEEE TRANSACTIONS ON INFORMATION THEORY. He is currently an Associate Editor of the *IMA journal on Information and Inference*, the *SIAM journal on Imaging Sciences*, the *IEEE Signal Processing Magazine*. He is ranked the World's Highly Cited Researchers of 2016 by Clarivate Analytics of Thomson Reuters.